Reflection-Type Hologram for Atoms

Fujio Shimizu
Institute for Laser Science and CREST, University of Electro-Communications, Chofu-shi, Tokyo 182-8585, Japan

Jun-ichi Fujita
NEC Fundamental Research Laboratories, 34 Miyukigaoka, Tsukuba 305-8501, Japan
(Received 16 November 2001; published 7 March 2002)

A cold metastable neon atomic beam was manipulated with a reflective amplitude hologram that was encoded on a silicon surface. A black-and-white pattern of atoms was reconstructed on a microchannel plate detector. The hologram used the enhanced quantum reflection developed by authors and was made of a two-dimensional array of rectangular low and high reflective cells. The surface of the high reflective cell was composed of regularly spaced roof-shaped ridges, while the low reflective cell was simply a flat surface. The hologram was the first demonstration of reflective atom-optical elements that used universal interaction between a neutral atom and solid surface.

DOI: 10.1103/PhysRevLett.88.123201 PACS numbers: 34.50.Dy, 03.75.–b, 34.20.Cf

For centuries optical instruments have developed relying mostly on the deflection and reflection of an optical wave from a solid surface. High accuracy of the surface preparation and precisely defined reflecting surface were the technical basis that enabled one to produce stable and highly accurate optical instruments. Manipulation of a particle beam, on the contrary, relied mostly on externally applied forces that extended many orders of magnitude longer than the de Broglie wavelength of the particle. Recent development on the laser cooling of neutral atoms made it possible to control atoms with weaker forces. Slow atoms were reflected near a solid surface by using evanescent light field on a glass surface [1,2] or by Zeeman potential on a magnetically poled surface [3]. In principle, an atom can be coherently reflected from a solid surface by naturally existing short-range repulsive potential. Focusing of a supersonic He beam by reflection from a curved silicon wafer was demonstrated [4]. However, a nearly diffraction-limited reflection has never been achieved with a natural solid surface. The reason is that a solid surface is not flat to atomic scale over macroscopic dimension, and the atom is scattered at steps of atomic scale. This situation is the same for cold atoms that have a long de Broglie wavelength. When an atom approaches the surface, it is accelerated by attractive van der Waals force and shrinks its wavelength before it hits the repulsive core potential.

However, it has been realized for some time that an atom can be reflected at the attractive van der Waals potential before it hits repulsive core potential. The reflection occurs as a result of wave vector mismatch due to the steep spatial variation of the potential and is called quantum reflection. Since the atom is reflected at some distance from the surface, irregularity of the surface is averaged out. In addition, the position of reflection is defined within a fraction of atomic de Broglie wavelength. These characteristics resemble closely the reflection of an optical wave from solid surface. Quantum reflection was experimentally verified first on helium and hydrogen atoms from a superfluid liquid helium surface [5–8]. We verified recently quantum reflection of a metastable neon atomic beam from a solid surface [9]. Nearly diffraction-limited reflection of an atomic beam of a 100 μm diameter was observed.

Although the reflectivity approaches unity as the normal incident velocity approached zero, it drops off rapidly as the velocity is increased. A peculiar feature of the quantum reflection is that the reflectivity is expected to become larger if the magnitude of the interaction energy gets smaller. It is easy to see from the one-dimensional Schrödinger equation of the atom interacting with the van der Waals potential $-C_3/z^3$ that the energy scales with $m^{-3}C_3^{-2}$ and the distance with mC_3, where m is the mass of the atom. Therefore, the reflectivity increases if the density of the solid near the surface is reduced. Motivated by this prediction, we etched the silicon surface to form the grating structure of parallel ridges with a narrow top so that the colliding atoms interacted only with a small fraction of the surface. We obtained a remarkable improvement on reflectivity, which encouraged us to design reflective coherent optical elements with quantum reflection [10]. This paper reports the first example of a practical atom-optical element that uses quantum reflection. A reflective amplitude hologram was fabricated on a silicon surface, where the ridged structure was used as high reflective area of the hologram. An ultracold neon atomic beam in the $1s_3(2p^5[1/2]^0 3s(J = 0))$ metastable state was diffracted from the hologram and formed a black and white pattern on the screen.

Experimental setup of the reflective atom holography shown in Fig. 1 was nearly the same as our previous report [10], except that the solid surface was not a uniform grating structure but was an amplitude hologram pattern. Neon atomic beam in the $1s_3$ metastable state was generated from atoms in the $1s_5(2p^5[3/2]^0 3s(J = 2))$ state in a magneto-optical trap by optical pumping through the $2p_5(2p^5[3/2]3p(J = 1))$ state. The $1s_3$ atoms fell nearly vertically and hit the hologram that was placed

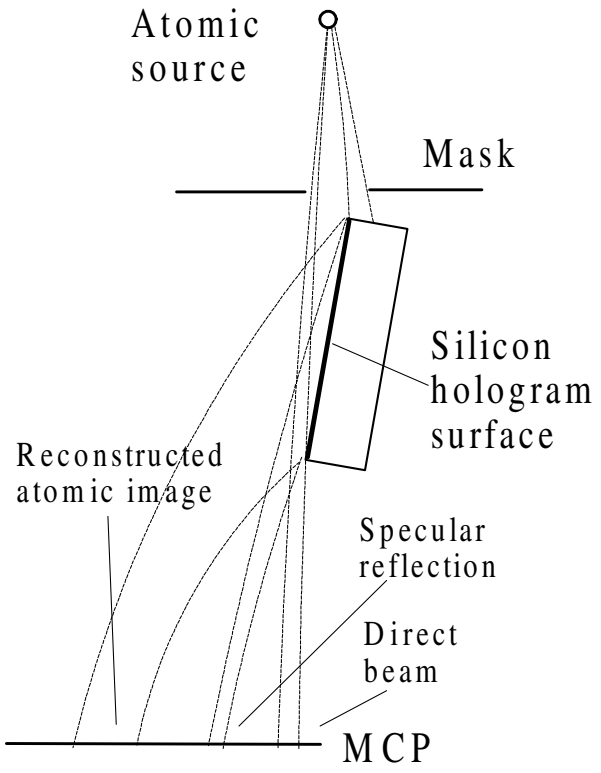

FIG. 1. Cross sectional view of the experimental setup.

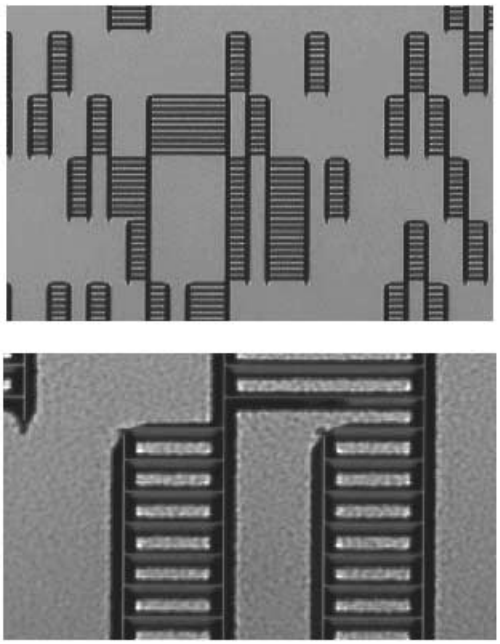

FIG. 2. Microscope photographs of a part of the hologram surface. The size of the cell was 100 μm vertically and 25 μm horizontally. It contained ten horizontal ridges and the vertical ridges at the boundary between high and low reflective cells. The vertical ridge protected the end of the horizontal ridge against erosion during the etching process.

approximately 44 cm below the trap. The angle of the hologram surface to the vertical line, θ, was typically a few milliradians. The reflected atom produced an interference pattern on a microchannel plate detector (MCP) that was placed 112 cm below the atomic source. In the following discussion we use (x, y) for the orthogonal coordinate on the hologram surface and (X, Y) for the image plane (MCP), where the x axis is parallel to the image plane, and the X and x axes are parallel.

The hologram used the $(0, 0, 1)$ silicon surface and was composed of rectangular cells with high or low reflectivity expressing a binary pattern. The low reflective cell was simply a flat surface. The high reflective cell was composed of regularly spaced roof-shaped ridges. The ridge was formed by the following procedure. A 100-nm-thick oxidized layer was formed on the surface, and then the surface was coated with a negative resist. A periodic pattern of 100-nm-wide stripes was written by an electron beam on the resist, and the oxidized layer excluding the stripe was removed photolithographically with buffered HF. The direction of the stripe was aligned precisely parallel to the $(1, 1, 0)$ or $(1, -1, 0)$ direction. The silicon was then etched with tetra-methyl-ammonium (TMAH). The etchant etched preferentially the $(0, 0, 1)$ surface and left $(\pm 1, \mp 1, 1)$ facets on two sides of the oxidized stripe, forming a roof-shaped ridge. The periodic ridge was placed parallel to the x axis. To protect the end of the ridge against erosion during the last etching process, the ridge of the same shape was formed along the vertical border that separated high and low reflective cells. Figure 2 shows a microscope photograph of a part of the hologram surface. The picture was focused on the top of the ridge, and white lines in the lower figure show the flat top of the ridge. The size of the cell was 25×100 μm^2, and a cell had ten parallel ridges. The height of the ridge was approximately 2 μm, and its top width 100 nm.

Although the ridged structure showed a remarkable improvement on reflectivity, θ had to be kept less than 10^{-2} rad to maintain sufficiently high reflectivity for the atomic pattern generation. With this small θ the hologram pattern cannot be calculated by Fourier transform of the object pattern as in the case of the transmission hologram placed perpendicular to the atomic beam [11]. We used a simplified algorithm described below. It was not a mathematically rigorous method. However, the result of numerical simulation was satisfactory, and it saved calculation time when the bright area of the object covered only a small fraction of the entire object plane. The complex amplitude of the atomic wave on the detector $F(X, Y)$ was obtained by integrating a contribution from the hologram surface (x, y),

$$F(X, Y) = A \iint f(x, y) \exp\{\imath \Phi(X, Y, x, y)\}\, dx\, dy\,, \quad (1)$$

where $f(x, y)$ was the amplitude reflectivity of the hologram and

$$\Phi = \int \frac{\boldsymbol{p}\, d\boldsymbol{r}}{\hbar}$$

was the integrated phase of an atom from the point source to the detector surface (X, Y) via the hologram surface

(x, y). The integral was carried out along the classical path of the atom, where $\boldsymbol{p}$ was its classical momentum. The rigorous hologram pattern could be obtained by solving the integral equation Eq. (1). We assumed that $f(x, y)$ required to obtain $F(X, Y)$ was the inverse integral of Eq. (1)

$$f(x, y) = A' \iint F(X, Y) \exp\{-\imath\Phi(X, Y, x, y)\}\, dX\, dY\,.$$

We divided the hologram into rectangular cells and chose an object that was composed of spots of equal brightness. Then, complex reflectivity of the (l, m) cell whose center was at (x_l, y_m) was

$$f(l, m) = A^{\dagger} \sum_n \frac{\sin(\Delta p_x d_x/\hbar)}{\Delta p_x} \exp(\imath\phi_n) \times \exp\left(-\imath\Phi(X_n, Y_n, x_l, y_m)\right), \qquad (2)$$

where d_x was the horizontal (x) length of the rectangular cell, Δp_x was the momentum jump of the atom on the hologram surface along x axis, and ϕ_n was a random phase multiplied on the nth spot of the object. The factor $\sin(\Delta p_x d_x/\hbar)/\Delta p_x$ arose from the integration within a cell and was equal to the amplitude of the atomic wave diffracted from a cell along the x axis. This factor was not necessary if the entire image were written within the area of diffraction from a single cell. In the experiment described below, the size of the image was larger than the diffraction limit along the X direction but was smaller along the Y direction. A similar factor was necessary along the y axis if the size of the image along the Y axis were larger. Finally, a threshold was set on the real part of $f(l, m)$ to make the hologram binary. Typically the threshold was 10% of the peak value of $\mathcal{R}f(l, m)$.

Figure 3 shows the experimental result. The object was the word "*SURFACE*" that was drawn with a series of dots separated by approximately 50 μm (top figure). The hologram consisted of approximately 250 cells along x and 1024 along y, and the size of the cell was 25×100 μm^2. The angle between the hologram surface and the incident atomic beam, θ, was set to 2.5 mrad. The middle figure shows approximately one-eighth of the hologram pattern. A cell was expressed by a square in the figure. The bottom figure shows the atomic pattern reconstructed on the microchannel detector. The thick strip in the lower part of the figure was the image of specularly reflected atoms (zeroth-order diffraction pattern). The thin longer stripe was produced by vacuum ultraviolet photons that were emitted from the atomic source during the optical pumping process. The data were accumulated for approximately 4 h. The image of the specular reflection contained approximately 4×10^5 atoms. The area of the reconstructed pattern contained 7×10^4 atoms. The number of atoms that hit the hologram was estimated from the density of atoms that hit the MCP directly from the atomic source and was 1.5×10^6. Therefore, a quarter of the atoms that hit the hologram were reflected specularly and 4% contributed to construct the image. The latter value was approximately a factor of 2 smaller than the theoretically attainable efficiency of an amplitude hologram.

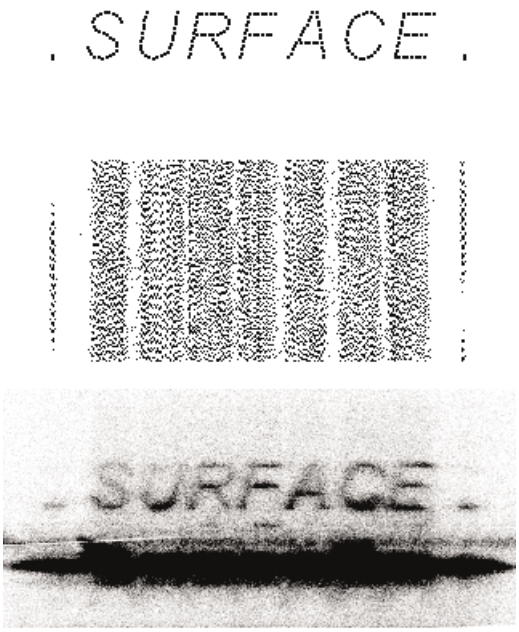

FIG. 3. The top figure is the object pattern, the middle is one-eighth of the hologram pattern, and the bottom figure is the reconstructed atomic image that was accumulated by the microchannel plate detector. The thick black line on the lower part of the figure was produced by specularly reflected atoms (zeroth-order pattern). The thin line was caused by vacuum ultraviolet photons that accompanied the optical pumping process in the atomic source. The hologram pattern of dots on two sides were rotated by 3 mrad. They produced line images that were used to check the angular alignment of the hologram.

The size of the atomic image shown in Fig. 3 was much larger than that limited by diffraction of an atomic wave from a single cell of the hologram. This was necessary, because it was not possible to make the high reflective cell smaller than the periodicity of the ridge. In Fig. 3 the atomic wave diffracted from a single cell covered 0.17 mm along the X axis and 4.8 mm along the Y axis. Therefore, while all cells along the y axis contributed to the construction of each image point, no more than the neighboring 7 cells along the x axis contributed to the same point. This caused the intensity variation on the image which depended on the number of bright spots along the Y axis. Since the threshold for the binary hologram pattern was set close to the average value of $f(l, m)$, the number of atoms integrated over a vertical line Y was roughly constant over X regardless of the number of bright spots of the object. Therefore, a larger number of atoms were concentrated on a smaller region when the number along the Y axis was small. The intensity variation could be corrected if a weighting function that was approximately equal to the square root of the number of bright spots along Y was multiplied in Eq. (2).

In conclusion, we have demonstrated for the first time a reflective atom-optical element that uses a universal

interaction between a neutral atom and a solid surface. In the present experiment the incident angle θ was limited to a small value. The reflectivity at a larger θ, or a faster normal incident velocity, will be improved if a surface with finer structure is used. The reflecting plane of the quantum reflection approaches the solid surface as the velocity is increased. The maximum velocity is limited from the minimum distance that dominates the van der Waals potential. Atom optics on earth with atoms slower than a m/s is not practical because of the gravity acceleration. As a result, for atoms heavier than neon, θ will be limited to a relatively small angle. However, because of the m^{-3} scaling law on kinetic energy, lighter atoms such as hydrogen or helium can be used practically at any angle if an adequate surface is provided. For those atoms quantum reflection will be a powerful mean to construct stable and highly accurate atom-optical instruments.

This work was partly supported by the Grants in Aid for Scientific Research (11216202) from the Ministry of Education, Science, Sports and Culture.

[1] V. I. Balykin, V. S. Letokov, Yu. B. Ovchinnikov, and A. I. Sidorov, Pis'ma Zh. Eksp. Teor. Fiz. **45**, 282 (1987) [JETP Lett. **45**, 353 (1987)]; Phys. Rev. Lett. **60**, 2137 (1988). See also V. Balykin, Adv. At. Mol. Opt. Phys. **41**, 181 (1999), and references therein.
[2] M. A. Kasevich, D. S. Weis, and S. Chu, Opt. Lett. **15**, 607 (1990).
[3] T. M. Roach, H. Abele, M. G. Bochier, H. L. Grossman, K. P. Zetie, and E. A. Hinds, Phys. Rev. Lett. **75**, 629 (1995). See also E. A. Hinds and I. G. Hughes, J. Phys. D **32**, R119 (1999), and references therein.
[4] B. Holst and W. Allison, Nature (London) **390**, 244 (1997).
[5] V. U. Nayak, D. O. Edwards, and N. Masuhara, Phys. Rev. Lett. **50**, 990 (1983).
[6] J. J. Berkhout *et al.,* Phys. Rev. Lett. **63**, 1689 (1989).
[7] J. M. Doyle *et al.,* Phys. Rev. Lett. **67**, 603 (1991).
[8] I. A. Yu *et al.,* Phys. Rev. Lett. **71**, 1589 (1993).
[9] F. Shimizu, Phys. Rev. Lett. **86**, 987 (2001).
[10] F. Shimizu and J. Fujita, J. Phys. Soc. Jpn. **71**, 5 (2002).
[11] M. Morinaga *et al.,* Phys. Rev. Lett. **77**, 802 (1996).